Biochimica et Biophysica Acta 862 (1986) 265–272
Elsevier

BBA 72944

Tryptophan interactions of gramicidin A′ channels in lipids: a time-resolved fluorescence study *

Lanfranco Masotti [a], Paolo Cavatorta [b], Giorgio Sartor [a], Emanuela Casali [a] and Arthur G. Szabo [c]

[a] *Institute of Biological Chemistry and* [b] *Department of Physics, University of Parma, 43100 Parma (Italy) and* [c] *Division of Biological Sciences, National Research Council of Canada, Ottawa, Ontario K1A OR6 (Canada)*

(Received 15 July 1986)

Key words: Ion channel; Gramicidin, Lipid–protein interaction; Tryptophan fluorescence; Stacking interaction

The evolution of the incorporation of cation transport channels into lysolecithin micelles by gramicidin A was followed by measuring the ns time-resolved fluorescence of the tryptophan residues. In all samples, the tryptophan fluorescence could be resolved into three exponentially decaying components. The three decay times ranged from 6 to 8 ns, 1.8 to 3 ns, and 0.3 to 0.8 ns, depending on the emission wavelength. The fractional fluorescence of each component changed with incubation time. The long lifetime component had a reduced contribution to the total fluorescence while the short decay time component increased. The fluorescence spectra could be resolved into three distinct fluorescent components having maxima at 340 nm, 330 nm and 323 nm after 90 min of incubation, and 335 nm, 325 nm and 320 nm after 24 h of incubation. These maxima were, respectively, associated with the long, medium and short decay components. The fluorescence decay behaviour was interpreted as representing three families of tryptophans, the short lifetime component being due to a stacking interaction between tryptophan residues. The variation with incubation time suggests a two-step process in the channel-lipid organization. The first is associated with the conformational change of the polypeptide as it takes up a left-handed helical head-to-head dimer structure in the lipid. The second step is proposed to involve changes originating from membrane assembly and intermolecular interactions between channels as they form hexameric clusters.

1. Introduction

An important feature of the living organism is the timely specific control of ionic movements. Cells, as a rule, do not allow ions to readily permeate their membranes. If particular ions are required by the cell or organelle, special pathways must be developed in the membranes in the form of specific channels. The antibiotic gramicidin A′ provides an example of such a channel. It does not function to increase the permeability of the parent cell membrane but rather that of membranes in other organisms, such as invading bacteria. Because of its availability and well-characterized features, gramicidin A′ has been widely used as a model for studying the molecular mechanisms of selective ion transport across membranes [1–6]. Extensive studies have been carried out on the conformation of the peptide, the active state of the channel, the mechanisms involved in the transport of ions, as well as on channel–channel and channel–lipid interactions. The active form of the

* Issued as NRCC No. 26494.

Correspondence: Dr. A.G. Szabo, Division of Biological Sciences, National Research Council of Canada, Ottaway, Ontario K1A OR6, Canada.

channel is a head-to-head dimer, linked by hydrogen bonding, which spans the membrane bilayer [4]. The dimer assumes a left-handed helical conformation [4,7] with an internal pore of about 4 Å in diameter which can accommodate monovalent cations [8]. The mechanism by which an ion moves through the channel has been shown to involve a libration of the carbonyl groups of the peptide backbone lining the hydrophilic interior of the pore [9]. The kinetics of ion transport fit a two site model and the binding of the ions has been shown to involve their coordination by the carbonyl groups of the tryptophan residues, 9, 11, 13 and 15 [10,11]. In studies with model phospholipid systems, such as lysophosphatidylcholine, it has been shown that associated with channel formation and aggregation within the lipid phase there is a reorganization of the phospholipid from a micellar to a bilayer structure [12]. During the process of incorporation of the channel in the lipid, a significant decrease of the quantum yield of tryptophan fluorescence was observed [13]. This indicates that the tryptophan residues play an important role not only in the mechanism of ion transport through the channel but also in the process of channel formation and organization of local lipid structure. In this paper, we report the results of studies in which the kinetics of incorporation and organization of the gramicidin A′ channel in lipids have been followed by time-resolved and static fluorescence and optical rotation measurements.

Materials and Methods

Gramicidin A′ was obtained from ICN Pharmaceuticals, Cleveland, OH, and used without further purification. Lysolecithin was purchased from Sigma Chemicals, St. Louis, MO. Its purity was checked by nuclear magnetic resonance spectroscopy and thin-layer chromatography. Double glass distilled water was used throughout the experiments.

Gramicidin A′ was added as a powder to a water suspension of phospholipid at a ratio of 1 : 4 (w/w) and the suspension was then sonicated for 10 min in a sonication bath. The resultant suspension was then heated for 24 h at 70°C, with continuous stirring. Small aliquots were withdrawn at different times and added to 2 ml of distilled water to give a final concentration of gramicidin A′ of about $1.3 \cdot 10^{-5}$ M.

All spectroscopic measurements were made at 20°C. Static fluorescence measurements were performed on a Perkin Elmer MPF-44A spectrofluorimeter equipped with a DCSU-2 corrected spectral unit. All spectra were corrected with excitation and emission bandpass of 2 nm each. The excitation wavelength was 280 nm. Fluorescence decay measurements and data analysis were performed as described [14]. The excitation source was a Spectra Physics dye laser system. Usually, fluorescence decay curves were measured until 50000 counts were accumulated in the maximum channel. The channel resolution was 42.6 ps/channel. The decay parameters were obtained after convolution using the delta function convolution method with terphenyl in ethanol as a reference material ($\tau_r = 1.10$ ns).

Fluorescence quantum yields were measured using *N*-acetyltryptophanamide (pH 7 buffer) as a quantum yield standard using a value of 0.14 for its quantum yield [15]. Absorbancies of the samples were adjusted to less than 0.05 at 280 nm.

Absorbance measurements were made on a Cary 219 spectrophotometer. When appropriate, an $\epsilon(281) = 2.25 \cdot 10^4$ mol^{-1}/cm in methanol was used to determine gramicidin A′ concentrations.

Circular dichroism measurements were carried out by means of a Jasco J-500A Spectropolarimeter, equipped with a microprocessor unit for spectra accumulation. The samples were measured using 0.2 mm pathlength cuvettes.

Results

The assembly of the membrane formed by gramicidin A′ and lysolecithin was followed using circular dichroism, static fluorescence and time resolved fluorescence measurements. Circular dichroism spectra recorded at 0, 15, 30 and 90 min during the incorporation of gramicidin A′ into lysolecithin are shown in Fig. 1. Clearly, significant conformational changes occurred even during the first 15 min. At 90 min gramicidin A′ had assumed the conformation which has been shown to be associated with the active state of the channel [16]. No further conformational changes were

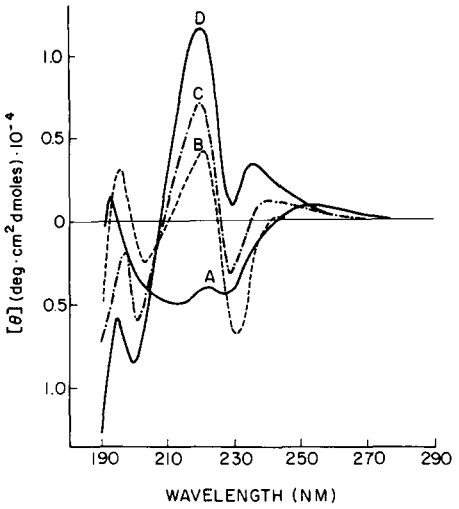

Fig. 1. Circular dichroism spectra of gramicidin A′ incubated with lysolecithin; A, 0 min; B, 15 min; C, 30 min; D, 90 min. Further changes were not observed after 90 min of incubation.

detected by circular dichroism measurements at longer times.

The fluorescence spectra associated with this gramicidin A′ incorporation are shown in Fig. 2. As the incubation time increased the fluorescence maximum shifted to higher energy, being 342 nm at 15 min and 90 min, and 328 nm at 24 h.

The blue shift of the fluorescence spectra with incubation time was accompanied by a decrease in the quantum yield as reported earlier [13]. The quantum yields have been revised, since in the earlier report scattered light at the excitation wavelength had not been accounted for. The quantum yield decreased from a value of 0.22 at 15 min incubation time to 0.07 at 24 h as shown in Fig. 3. The quantum yield at zero time could not be estimated with any degree of accuracy owing to the lack of solubility of gramicidin A′ in water. The absorbance of the sample increased with time. This was due to the increased solubilization of gramicidin A′ as the incorporation proceeded. The contribution of scattered light to the absorbance was accounted for by extrapolation from the scattered signal above 320 nm. The contribution of scattered light to the fluorescence was not important. This was shown by measuring the scattered light intensity, under identical conditions as the gramicidin A′ sample, of a glycogen suspension which had an absorbance at 340 nm equivalent to that of the gramicidin A′-lipid sample. As reported earlier neither thermal nor photo-decomposition of gramicidin A′ occurred during peptide incorporation [13].

The fluorescence decay parameters of the gramicidin A′-lysolecithin samples were measured at several wavelengths between 315 nm and 380 nm (excitation at 295 nm). The decay profile (Fig. 4a) measured at 335 nm for the 90 min incubation time sample shows that the decay kinetics could not be fit with a single exponential function. Judging by a random distribution of residuals in a

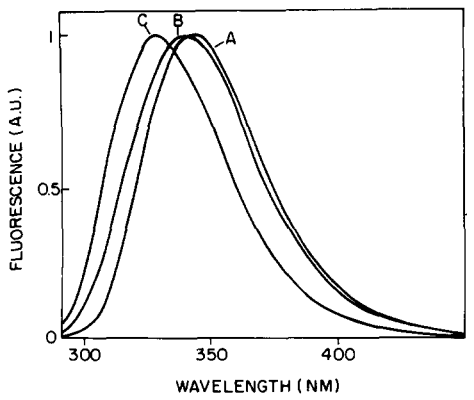

Fig. 2. Corrected fluorescence emission spectra of gramicidin A′ during incubation with lysolecithin. A, 0–60 min; B, 4 h; C, 24 h ($\lambda_{ex} = 280$ nm). A phospholipid blank was subtracted from each spectrum.

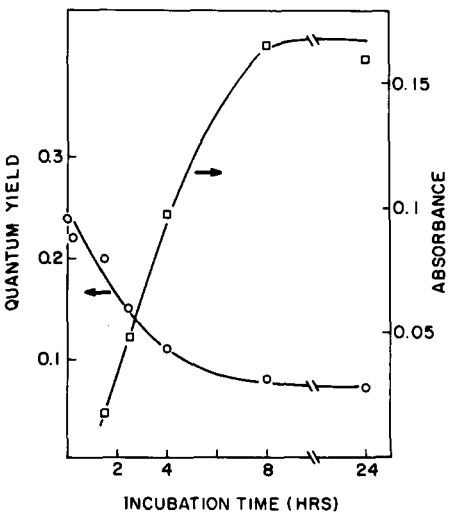

Fig. 3. Variation of quantum yield of fluorescence (○) and absorbance (□) of gramicidin A′ during incorporation with lysolecithin.

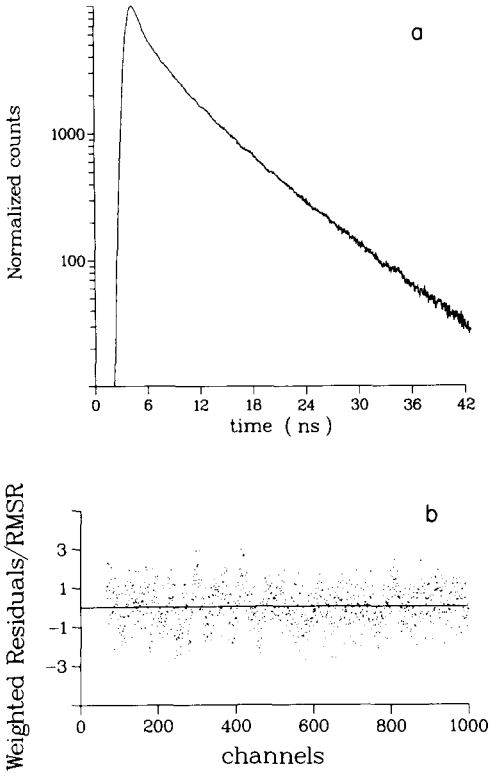

Fig. 4. (a) Fluorescence decay profile measured at 325 nm for the sample incubated for 90 min (channel width: 0.021 ps; $\lambda_{ex} = 295$ nm). (b) Plot of weighted residuals for the best-fit three exponential decay function.

weighted residual plot (Fig. 4b) and other statistical parameters, the decay data was satisfactorily fit to three exponential decay components. The decay times were different at different wavelengths. For example, at 90 min incubation, the fluorescence measured at 335 nm had decay times of 7.8 nm, 2.7 ns and 0.60 ns. At 380 nm the same sample had decay times of 8.3 ns, 3.7 ns, and 1.2 ns. The variation of decay times with emission wavelength is summarized in Fig. 5. The value of the decay times at different incubation times at any particular wavelength remained relatively constant (Fig. 6) except that there was a small decrease in the value of the medium decay time with incubation time.

There was a more perceptible variation in the pre-exponential terms with incubation time. This variation at 335 nm and 380 nm is shown in Fig. 7. A similar variation was observed at other wave-

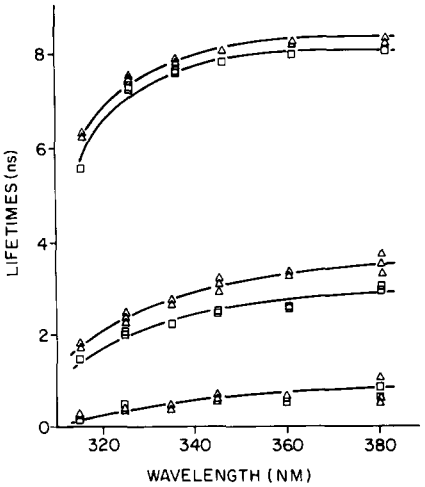

Fig. 5. Variation of fluorescence decay times with emission wavelength for 90 min (△) and 24 h (□) incubation.

lengths. The pre-exponential terms associated with the short decay time component and long decay time component varied with the incorporation time: the value of the former increased while the latter decreased. The pre-exponential term of the medium decay time component remained constant.

The variation in decay time and pre-exponential terms could be related to the changes in the fractional fluorescence contribution of each com-

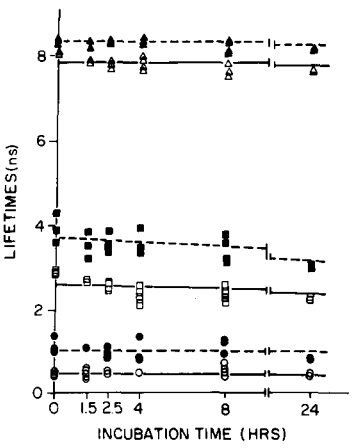

Fig. 6. Variation of fluorescence decay times with incubation time. Emission wavelengths were 335 nm (open symbols) and 380 nm (closed symbols). Lifetimes were short (○,●), medium (□,■) and long (△,▲).

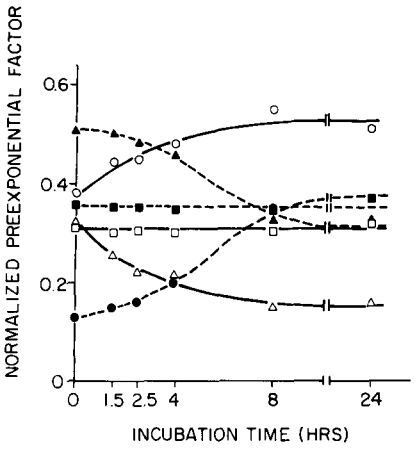

Fig. 7. Dependence of normalized pre-exponential factors on incubation time. Symbols for emission wavelength and lifetimes are the same as those in Fig. 6.

ponent according to the following relationship:

$$F_i = \alpha_i \tau_i / \sum_{n=1}^{j} \alpha_i \tau_i$$

where F_i, α_i, τ_i are the fractional fluorescence, pre-exponential term, and decay time of the ith component, respectively. This variation with incubation time is shown in Fig. 8. The fractional fluorescence of the short and medium decay components were seen to increase with time, while the long decay component decreased with incubation time. Apparently, after 8 h of incubation the fractional fluorescence of all components remained nearly constant.

From the fractional fluorescence values at each wavelength it was possible to resolve the fluorescence spectrum of incorporated gramicidin A′ at any incubation time into three spectral components. This was done for the 90-min and 24-h incubation samples and the time-resolved fluorescence spectra are shown in Fig. 9. The spectra of the 90 min sample had the maxima of the long, medium and short decay time components positioned at 340 nm, 330 nm and 323 nm, respectively. For the 24-h sample the maxima had all shifted to higher energy and were, respectively, found at 335 nm, 325 nm and 320 nm. The increased importance at 24 h of the two lower-value decay components to the total fluorescence which was first suggested in Fig. 8 is now clearly represented.

It is noted that the measurements presented in this work were made on samples which were dilutions (×40) of the original incorporation. Experiments performed at other dilutions gave similar results indicating that the structure of the complexes were not altered significantly with dilution.

Earlier, it has been reported [17] that the fluorescence spectrum of gramicidin A′ in dioxane was

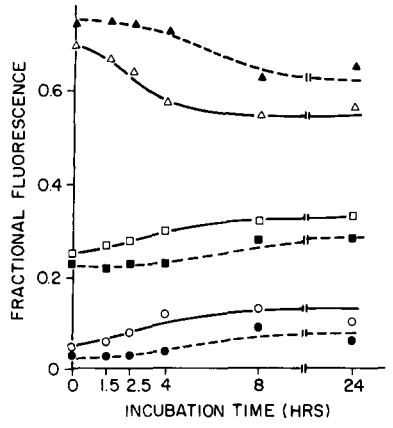

Fig. 8. Variation of fractional fluorescence with incubation time. Symbols for emission wavelength and lifetimes are the same as those in Fig. 6.

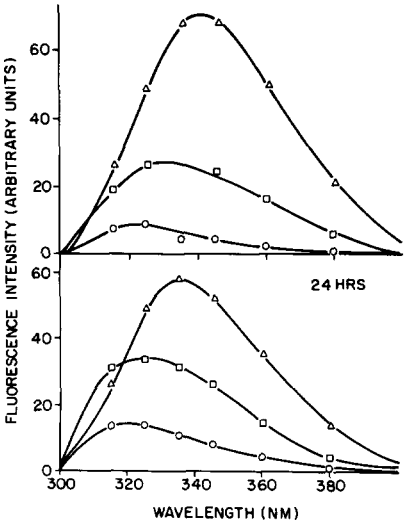

Fig. 9. Time-resolved emission spectra of gramicidin A′ incubated with lipid for 90 min (top) and 24 h (bottom) (emission bandpass: 4 nm). Lifetimes: ○, short; □, medium; and △, long.

similar to the final spectrum observed in lysolecithin. The fluorescence spectrum in methanol is similar to the spectrum of gramicidin A′ at very early incubation times. We considered that time resolved fluorescence measurements of gramicidin A′ in these solvents might provide relevant information on the gramicidin A′-lysolecithin complex. However, the decay parameters obtained in these solvents depended on the history of the samples (age, concentration). This is probably due to the complex equilibria between the various gramicidin peptides reported by Veatch and Blout [18].

Discussion

The circular dichroism data show that gramicidin A′ undergoes conformational changes during the first 90 min of incubation with lysolecithin and during this time, as shown in Fig. 1, more and more polypeptide becomes incorporated into the lipid structure. After this time, gramicidin A′ attained a left-handed helical conformation which remained stable with time and can be associated with the active state of the channel [16]. It is therefore possible to associate the changes in quantum yield, fluorescence lifetimes and pre-exponential factors observed in the first 90 min mainly to conformational changes of the polypeptide, that is to say to intramolecular interactions. Any change in the spectroscopic properties of the Trp residues monitored afterwards should then be associated with intermolecular side-chain interactions taking place during the process of membrane assembly and cluster formation.

While trying to rationalize the fluorescence data, one has to bear in mind two main facts. First, the channel assumes a triangular structure where Trp 11 and Trp 13 each occupy different apexes and Trp 9 and Trp 15 share the remaining apex and are stacked [17,19,20]. Second, the polypeptide orientation in the lipid layer is one in which the formyl end is buried deeply within the bilayer and the ethanolamine end is exposed to the external environment [21].

The fluorescence results can safely be solely attributed to gramicidin A′ which has been incorporated into lysolecithin micelles. Gramicidin A′ is totally insoluble in aqueous buffers and hence free gramicidin A′ may be discounted as contributing to the fluorescence decay heterogeneity. The gramicidin A′-lysolecithin system may consist of complexes having different quantities of gramicidin and the lifetime heterogeneity may be thought to be attributed to such a possibility. However, we do not consider that the quantity of gramicidin A′ in the micelles significantly affects the results, since results at different dilutions were similar. Further studies are planned to clarify this point. For the present we interpret the results in terms of an ensemble average of the gramicidin A′-lysolecithin system.

The fluorescence decay behaviour is best described by triple exponential decay kinetics in every case. As shown in Fig. 6 the value of the decay times vary slightly with incubation time. Also, the decay time for a given incubation time varies with emission wavelength and indeed the fluorescence can be resolved into three distinct spectral components, with max 340, 330, 323 nm at 1.5 h of incubation and 335, 325, 320 nm at 24 h of incubation. For this reason, one must be cautious in assigning a particular decay time to a specific tryptophan residue. In the subsequent rationalization we favour an interpretation in which each decay and spectral component can be assigned to different families of tryptophans. The one family has a decay time ranging from 6 to 8 ns, depending on the emission wavelength; a second family with a decay time range of 1.8–3 ns; and a third family having values between 0.3 ns and 0.8 ns. The observation that during incubation the integrated fluorescence of the long lifetime class was reduced while that of the short and medium components increased, provides additional support for the above interpretation.

The long lifetime component may be attributed to tryptophans deeply buried in the lipid, and the medium component to tryptophans experiencing an environment in which deactivation processes, such as those that would occur in a region near the membrane surface, would become more important. The short lifetime component, on the other hand, could be due to the stacking interactions of two Trp residues, e.g., Trp 9 and Trp 15, at early times of incubation [17]. The decay time of the tryptophans in this stack may be shortened because of exciton interactions between the indole rings. Such an exciton interaction has been ob-

served in circular dichroism studies [7]. Alternatively, it is generally accepted that the lowest singlet state of the indole ring of the tryptophan residue has considerable charge transfer character [22]. Interactions between the excited state dipole of this charge transfer state with the ground state dipole of a stacked neighbouring indole ring would result in enhanced excited state deactivation processes resulting in a shorter lifetime.

Consistent with this latter view is the observation that within each class there is a wavelength dependence of the decay time. This may result from dielectric relaxation induced by the excited state dipole of the tryptophan residues. At early incubation times such a relaxation would result from intramolecular interactions while at long incubation times there is the additional possibility of intermolecular interactions, such as may occur in the formation of cluster [17].

The increase in intermolecular interactions during incubation time is confirmed by several observations. The fluorescence quantum yield decreased, and the normalized pre-exponential factors and the fractional fluorescence of each component varied with incubation time (Figs. 3, 7 and 8). The increase of the pre-exponential factor of the short decay time component and the decrease of that of the long lifetime component indicate a conversion of the latter class into the former, at increasing incubation time. The pre-exponential factor for the medium lifetime component remained constant with time. A possible explanation for this observation is that for the assembly of the clusters and their organization in rows, Trp 11–Trp 13 interactions from different dimers either by stacking or by close contact are required. This leads to an increase in the weight of the class of Trp residues whose decay time is centered at the shortest value. By integration of the areas of the time-resolved spectra of Fig. 9, it was possible to show that the ratio of the short-to-long lifetime components changed from 1.6 at 1.5 h to 3.4 at 24 h. Concomitantly, there was an increase of the ratio of the medium to long lifetime components by a factor of 1.4 and a 1.5-fold increase of the ratio of short-to-medium lifetime components over the same time period.

At the same time, the fluorescence emission maxima of the three components shifted to higher energies explaining the blue shift of the total emission spectrum with incubation time shown in Fig. 2.

It should be kept in mind that gramicidin A′ is a mixture of 85% form A, with four tryptophan residues, 10% form B, substituted at residue 11 with a phenylalanine residue, and 5% C, with a tyrosine at residue 11. Nevertheless, in conclusion, we think that the time-resolved fluorescence studies reported in this paper give a reasonable picture of the dynamics involved in the assembly of the lipid system formed by the gramicidin A′ channels and lysophosphatidylcholine reported earlier [12, 13,17]. Two independent observations seem to indicate a particularly important role of tryptophan residues in the molecular mechanism of ion conductance and lipid channel assembly. It has been shown that the carbonyls of tryptophan residues 11 and 13, with a minor participation of those of residues 9 and 15, constitute the binding site for the movement of the monovalent ions through the channel. Substitution of the tryptophan residues in the gramicidin A′ molecule leads to the inability of the molecule to form bilayers with lysolecithin (Masotti et al., unpublished results). The results reported in this work further implicate the important involvement of the tryptophan residues in lipid–channel and channel–channel interactions during the assembly of the active membranous system under the conditions of our experiments.

Further studies, now in progress, with single molecular species of gramicidin and with liposomes from different phospholipids should provide a better insight into the mechanisms of packaging of the channels and clarify the role of tryptophan in the process.

Acknowledgements

The authors acknowledge the financial assistance of The National Research Council of Canada; National Science and Engineering Research Council; The NATO Scientific Affairs Division; and The Consiglio Nationale di Recherche, Italy (grant No. 84.01757.04/115.02180) and wish to thank Mr. D. Krajcarski for his expert technical assistance.

References

1 Hladky, S.B. and Haydon, D.A. (1970) Nature 225, 451–453
2 Hladky, S.B. and Haydon, D.A. (1971) Symposium of Molecular Mechanisms of Antibiotic Action on Protein Biosynthesis and Membranes (Munoz, E., Garcia-Fernandiz, F. and Vasquez, V., eds.), pp. 738–753, Elsevier Amsterdam
3 Goodall, M.C. (1970) Biochim. Biophys. Acta 219, 471–478
4 Urry, D.W. (1971) Proc. Natl. Acad. Sci. USA 68, 672–676
5 Bamberg, E. and Lauger, P. (1973) J. Membrane Biol. 11, 177–194
6 Veatch, W.R., Mathies, R. Eisenberg, M. and Stryer, L. (1975) J. Membrane Biol. 99, 75–92
7 Masotti, L., Spisni, A. and Urry, D.W. (1980) Cell Biophys. 2, 241–251
8 Urry, D.W., Goodall, M.C., Glickson, J.D. and Myers, D.F. (1971) Proc. Natl. Acad. Sci. USA 68, 1907–1911
9 Urry, D.W. (1973) in Conformation of Biological Molecules and Polymers (Jerusalem Symposium on Quantum Chemistry and Biochemistry), Vol. 5, p. 723, Israel Academy of Sciences, Jerusalem
10 Urry, D.W., Venkatachalam, C.M., Spisni, A., Lauger, P. and Khaled, M.A. (1980) Proc. Natl. Acad. Sci. USA 77, 2028–2032
11 Urry, D.W., Walker, J.T. and Trapane, T.L. (1982) J. Membrane Biol. 69, 225–231
12 Pasquali-Ronchetti, I., Spisni, A. Casali E., Masotti, L. and Urry, D.W. (1983) Biosci. Rep. 3, 127–133
13 Cavatorta, P., Spisni, A., Casali, E., Lindner, L., Masotti, L. and Urry, D.W. (1982) Biochem. Biophys. Acta 689, 113–120
14 Zuker, M., Szabo, A.G., Bramall, L., Krajcarski, D.T. and Selinger, B. (1985) Rev. Sci. Instrum. 56, 14–22
15 Chen, R.F. (1967) Anal. Lett. 1, 35
16 Urry, D.W., Spisni, A., Khaled, M.A., Long, M.M. and Masotti, O. (1979) Int. J. Quantum Chem. (Quantum Biology Symposium) 6, 289–303
17 Spisni, A., Pasquali-Ronchetti, I., Casali, E., Lindner, L., Cavatorta, P., Masotti, L. and Urry, D.W. (1983) Biochim. Biophys. Acta 732, 58–68
18 Veatch, W.R. and Blout, E.R. (1974) Biochem. 13, 5257–5264
19 Urry, D.W., Long, M.M., Jacobs, M. and Harris, R.D. (1975) Ann. N.Y. Acad. Sci. 264, 203–220
20 Mazet, J.L., Andersen, O.S., Koeppe, R.E. (1984) Biophys. J. 45, 263–276
21 Weinstein, S., Wallace, B.A., Blout, E.R., Morrow, J.S. and Veatch, W. (1979) Proc. Natl. Acad. Sci. USA 76, 7230–7234
22 Meech, S.R., Phillips D. and Lee, A.G. (1983) Chem. Phys. 80, 317–328